Antiangiogenic Role of Somatostatin Receptor 2 in a Model of Hypoxia-Induced Neovascularization in the Retina: Results from Transgenic Mice

Massimo Dal Monte,[1] *Maurizio Cammalleri,*[1] *Davide Martini,*[1,2] *Giovanni Casini,*[2] *and Paola Bagnoli*[1]

Purpose. To determine whether the somatostatin receptor 2 (sst_2) influences angiogenesis and its associated factors in a model of hypoxia-induced retinal neovascularization.

Methods. sst_1-knockout (KO) mice, in which sst_2 is overexpressed and overfunctional, and sst_2-KO mice were used. Angiogenesis was evaluated in fluorescein-perfused retinas. Angiogenesis-associated factors were determined by RT-PCR and immunohistochemistry.

Results. Retinal neovascularization was increased in sst_2-KO mice, but remained unchanged in sst_1-KO compared with wild-type (WT) mice. Retinal levels of sst_2 mRNA were not affected by hypoxia. Normoxic levels of angiogenesis regulators were similar in WT and KO retinas except for mRNA levels of IGF-1, Ang-2, and its receptor Tie-2. In WT, hypoxia induced an increase in mRNA levels of (1) VEGF and its receptors, (2) IGF-1R, and (3) Ang-2 and Tie-2. The increase in VEGF and IGF-1R mRNAs was more pronounced after sst_2 loss, but was less pronounced when sst_2 was overexpressed. In addition, in hypoxic retinas, sst_2 loss increased IGF-1 mRNA, whereas it decreased Ang-1, Tie-1, and Tie-2 mRNA levels. Moreover, Tie-1 mRNA increased when sst_2 was overexpressed. Immunohistochemistry confirmed the results in hypoxic retinas on increased expression of VEGF, IGF-1, and their receptors after sst_2 loss. It also allowed the localization of these factors to specific retinal cells. In this respect, VEGFR-2, IGF-1, and IGF-1R were localized to Müller cells.

Conclusions. These results suggest that sst_2 may be protective against angiogenesis. The immediate clinical importance lies in the establishment of a potential pharmacological target based on sst_2 pharmacology. (*Invest Ophthalmol Vis Sci.* 2007;48:3480–3489) DOI:10.1167/iovs.06-1469

The abnormal formation of new blood vessels characterizes a variety of retinal diseases, including diabetic retinopathy,[1] and requires the involvement of vascular endothelial growth factor (VEGF), insulin-like growth factor (IGF)-1, and their receptors VEGFR-1, VEGFR-2, and IGF-1R. Although the available information on their expression in the retina is far from being exhaustive, these factors have been localized to both retinal cells and microvascular endothelium.[2–6] Retinal neoangiogenesis is always associated with an increase of VEGF and its receptors[2,3,7] but not of IGF-1.[8–10] Of the other downstream factors affecting blood vessel growth, recent results indicate that Ang-1 and -2 and their tyrosine kinase receptor Tie-2 are regulated by hypoxia and play a role in retinal neovascularization.[11,12] Although a ligand for Tie-1 has not been found, it has recently been demonstrated that Ang-1 can induce Tie-1 phosphorylation.[13]

The potential antiangiogenic role of the peptide somatostatin-14 (SRIF) and its analogues has received much attention,[14] and it involves partial correction of systemic growth hormone dysregulation or inhibition of angiogenesis-associated factors.[15–17] Of the five SRIF receptors mediating SRIF actions, sst_2 is a likely candidate to mediate the angioinhibitory activity of SRIF. Indeed, analogues with high affinity for sst_2, such as octreotide and BIM23027, counteract the growth factor–induced proliferation of bovine retinal endothelial cells under hypoxia.[18] They are powerful inhibitors of neovascularization in models of proliferative retinopathies.[15,19] In addition, octreotide inhibits the IGF-1-mediated induction of VEGF in human retinal pigment epithelial (RPE) cells.[16] Moreover, octreotide retards retinopathy progression in diabetic patients in whom photocoagulation has failed.[20] However, despite the growing use of sst_2 agonists as antiangiogenic agents, the mechanisms by which these peptides inhibit the growth of new vessels has not been fully delineated.

Both sst_1- and sst_2-knockout (KO) mice have been generated.[21,22] In their retinas, we have found that sst_1 loss causes an increased expression and function of sst_2.[23–28]

In the present study, retinas of sst_1- and sst_2-KO mice were rendered hypoxic and were used to investigate whether altered levels of sst_2 play a role in regulating retinal angiogenesis and its associated factors. Our hypothesis was that, compared with wild-type (WT) retinas, the lack of sst_2 is associated with heavier effects of hypoxia, whereas a chronic overexpression of sst_2 (as in sst_1-KO retinas) should attenuate these effects.

Methods

Animals

Experiments were performed on 128 mice of WT (C57BL/6) and sst_1- or sst_2-KO strains of both sexes at postnatal day (PD)17 (6 g body weight). In some experiments designed to evaluate development of retinal vasculature, five PD12 mice for each strain were also used. sst_1- and sst_2-KO mice were generated as previously reported.[21,22] Experiments were performed in agreement with the ARVO Statement for the Use of Animals in Ophthalmic and Vision Research and in compliance with the Italian law on animal care 116/1992 and EEC/609/86. All efforts were made to reduce the number of animals used.

From the [1]Dipartimento di Biologia, Università di Pisa, Via san Zeno, Pisa, Italy; [2]Dipartimento di Scienze Ambientali, Università della Tuscia, Largo dell'Università, Viterbo, Italy.

Supported by Grant 2005052312 from the Italian Ministry of University and Research (MUR, PRIN) and Grant 2006-0146 Fondazione Cassa di Risparmio di Volterra.

Submitted for publication December 12, 2006; revised March 8, 2007; accepted May 21, 2007.

Disclosure: **M. Dal Monte**, None; **M. Cammalleri**, None; **D. Martini**, None; **G. Casini**, None; **P. Bagnoli**, None

The publication costs of this article were defrayed in part by page charge payment. This article must therefore be marked "*advertisement*" in accordance with 18 U.S.C. §1734 solely to indicate this fact.

Corresponding author: Paola Bagnoli, Dipartimento di Biologia, Università di Pisa, Via san Zeno, 31, 56127 Pisa, Italy; pbagnoli@biologia.unipi.it.

Investigative Ophthalmology & Visual Science, August 2007, Vol. 48, No. 8

Model of Hypoxia-Induced Retinopathy

In a typical model of hypoxia-induced retinopathy,[29] litters of mouse pups with their nursing mothers were exposed to a high oxygen concentration (75% ± 2%) between PD7 and PD12 in an infant incubator. Oxygen was checked twice daily with an oxygen analyzer (Miniox I; Bertocchi srl Elettromedicali, Cremona, Italy). After exposure to room air between PD12 and PD17, the mice were anesthetized by intraperitoneal injection of Avertin (1.2% tribromoethanol and 2.4% amylene hydrate in distilled water, 0.02 mL/g body weight; Sigma-Aldrich, St. Louis, MO). Mice kept in room air were used as control animals. All experiments were performed at the same time of day, to exclude possible circadian influences. The data were collected from both males and females and the results combined, as there was no apparent gender difference.

Assessment of Retinal Vascularization

Fluorescein-conjugated dextran perfusion of the retinal vessels was performed as previously described.[30] Briefly, animals were anesthetized, a median sternotomy was performed, and the left ventricle was perfused with 2 mL of a 25-mg/mL solution of fluorescein-conjugated dextran (Sigma-Aldrich) in 0.15 M phosphate buffer (PB). The eyes were enucleated, the retinas were dissected, and flatmounts were obtained. They were viewed by fluorescence microscopy (Eclipse E800; Nikon, Badhoevedorp, The Netherlands), and images were acquired (DFC320 camera; Leica Microsystems, Heidelberg, Germany). For the evaluation of retinopathy, we considered separately the formation of new vessels and the extent of loss of vessels in the central retina. Neovascularization was evaluated with the retinopathy scoring system shown in Table 1. Three trained observers evaluated the number of clock hours with abnormal vessels for each retina ($n = 12$ for each strain). The data were averaged and are expressed in values ranging from 0 to 8. A higher score indicates more severe retinopathy. For evaluation of the avascular area, we used a method previously described.[7] The avascular area and the total retinal area were measured in retinal images ($n = 12$ for each strain) with computer-assisted analysis (Axiovision 4 software; Carl Zeiss Vision GmbH, München-Hallbergmoos, Germany). For measurement of the capillary-free area, blind-coded retinal flatmounts were analyzed. Data are expressed as the percentage of the avascular area in relation to the total area. A direct comparison between aberrant retinal vessels revealed by fluorescein angiography and histologic cross sections (10-μm thick) was performed in the flatmounts used for retinopathy evaluation.

Measurements of mRNA Levels by Semiquantitative RT-PCR

RT-PCR in mouse retinas ($n = 8$ for each strain) was performed as previously described.[27] Briefly, anesthetized mice were killed by cervical dislocation, and the eyes were rapidly removed. After removal of the anterior segments, dissected retinas were homogenized in extraction reagent (TRIzol; Invitrogen, Carlsbad, CA). First-strand cDNA was generated from 1 μg of total RNA, and one tenth of the RT product was amplified in a total volume of 25 μL, using 1.25 U *Taq* polymerase. mRNAs of angiogenesis-associated growth factors and their receptors were coamplified with S16 mRNA whereas sst_2 mRNA was coamplified with cyclophilin B mRNA in an automatic thermocycler (Bio-Rad, Hercules, CA). Both cyclophilin B mRNA and S16 mRNA were used as internal standards. Forward and reverse primers were chosen from mouse sequences and are listed in Table 2. A 20-μL sample of the PCR reaction was electrophoresed on a 4% agarose gel (Eurobio, Les Ulis, France) and stained (GelStar; BMA, Rockland, ME). After migration, bands corresponding to the amplified products were analyzed (Gel Doc 2000 System equipped with Quantity One software; Bio-Rad). For semiquantitative analysis of the PCR products, we measured the signal intensity of the bands with respect to intensity of the signal for either S16 or cyclophilin B in the same lane (mRNA/S16 mRNA or mRNA/cyclophilin B mRNA).

Immunohistochemistry

Immunohistochemistry was performed in the retinas of three anesthetized mice for each strain and killed by cervical dislocation. The eyes were removed and immersion fixed in 4% paraformaldehyde in 0.1 M PB (pH 7.4) for 1 hour. The fixed eyes were transferred to 25% sucrose in 0.1 M PB and stored at 4°C. Retinal sections were cut perpendicular to the vitreal surface at 10 μm with a cryostat, mounted on gelatin-coated slides, and stored at −20°C. Primary rabbit antisera directed to VEGF, VEGFR-1, VEGFR-2, IGF-1 (1:100 dilution), and the β subunit of IGF-1R (1:30 dilution; Santa Cruz Biotechnology, Santa Cruz, CA) were used. In double-labeling experiments, a mouse monoclonal antibody directed to glutamine synthetase (Chemicon, Temecula, CA) was also used as a Müller cell marker[34] at 1:500 dilution in conjunction with VEGFR-2, IGF-1, and IGF-1R antibodies. Goat anti-rabbit and anti-mouse secondary antibodies conjugated with Alexa Fluor 488 or Alexa Fluor 546 (Invitrogen-Molecular Probes, Eugene, OR) were used at a dilution of 1:200. Control experiments included the omission of the primary antibodies. Nonspecific staining was not observed. Immunofluorescence images were acquired with a 40× objective, a digital camera (Plan-Neofluar Zeiss Axiocam MRC; Carl Zeiss Meditec, GmbH) connected to an epifluorescence microscope, and software (Axiovision 4; Carl Zeiss Meditec, GmbH). The digital images were sized and optimized for contrast and brightness (Photoshop 5.0; Adobe Systems, Mountain View, CA). Final images were saved at a minimum of 300 dpi.

Statistical Analysis

Data were analyzed by the Kolmogorov-Smirnov test on verification of normal distribution. Statistical significance was evaluated with ANOVA followed by the Newman-Keuls multiple comparison post test (Prism; GraphPad Software, San Diego, CA). Numerical data are expressed as the mean ± SE. Differences with $P < 0.05$ were considered significant.

Results

Retinal Neovascularization

In both WT and KO retinas, exposure to 75% ± 2% oxygen between PD7 and PD12 resulted in the disappearance of existing capillaries in the central retina, although the peripheral

Table 1. Retinopathy Scoring System

	Points				
Criteria	**0**	**1**	**2**	**3**	**4**
Blood vessel tufts	None	In <3 clock hours	In 3–5 clock hours	In 6–8 clock hours	In 9–12 clock hours
Blood vessel tortuosity	None	<1/3 of vessels	1/3–2/3 of vessels	>2/3 of vessels	
Retinal hemorrhage	Absent	Present			

Flat-mounted retinas were examined by fluorescence microscopy and retinopathy was quantified by evaluating three criteria. Points received for each criterion were summed to obtain the retinopathy score. A higher score (range, 0–8) indicates more severe retinopathy. The scoring system was adapted from Higgins et al.[31]

TABLE 2. Primers used for RT-PCR analysis

Gene	Primer Sequence	Product Length (bp)	Ref.
sst$_2$	Forward: ATCAGTCCCACCCCAGCCCTGAA Reverse: GGGGTTGGCGCAGCTGTTG	76	Dal Monte et al.[27]
VEGF	Forward: CAGGCTGCCTGTAACGATGAA Reverse: AAAAACGAAAGCGCAAGAAA	221	Designed by Primer3 software[32]
VEGFR-1	Forward: TCGGCTGCAGTGTGTAAGTC Reverse: TGTCCCTTTTCCCACAAAAG	201	Ida et al.[33]
VEGFR-2	Forward: AGCTCTCCGTGGATCTGAAA Reverse: TAAGGGCATGGAGTTCTTGG	198	Ida et al.[33]
IGF-1	Forward: TGGATGCTCTTCAGTTCGTG Reverse: GGGAGGCTCCTCCTACATTC	351	Designed by Primer3 software[32]
IGF-1R	Forward: CAAGCTGTGTGTCTCCGAAA Reverse: GACCTGGAAGAACCGAATCA	161	Designed by Primer3 software[32]
Ang-1	Forward: AGGCTTGGTTTCTCGTCAGA Reverse: CCTTTTTGGGTTCTGGCATA	278	Designed by Primer3 software[32]
Ang-2	Forward: TCTTGGCCTCAGCCTACAGT Reverse: TTTGTGCTGCTGTCTGGTTC	375	Designed by Primer3 software[32]
Tie-1	Forward: CATCGAGACTTTGCAGGTGA Reverse: AGAAAGGCCAAAGTCTGCAA	363	Designed by Primer3 software[32]
Tie-2	Forward: TCAAGAAGGATGGGTTACGG Reverse: GCAAAAGCAGGGTCTGTCTC	253	Designed by Primer3 software[32]
Cyclophilin B	Forward: CCATCGTGTCATCAAGGACTTCAT Reverse: TTGCCATCCAGCCAGGAGGTCT	216	Dal Monte et al.[27]
S16	Forward: ATATTCGGGTCCGTGTGAAG Reverse: TCAAAGGCCCTGGTAGCTTA	85	Designed by Primer3 software[32]

retina remained vascularized (data not shown). Recovery in room air until PD17 allowed revascularization of the central avascular portion with associated marked neovascularization at the border between the central avascular and peripheral vascularized retina. Figure 1 shows the vascular pattern of flatmounts under normoxic (Fig. 1A–C) and hypoxic (Figs. 1D–F) conditions from WT (Figs. 1A, 1D), sst$_1$-KO (Figs. 1B, 1E), and sst$_2$-KO (Figs. 1C, 1F) mice. No differences were observed among normoxic WT and KO retinas. In both WT and KO mice returned to room air after exposure to high oxygen concentration, the central loss of blood vessels and the formation of engorged vessel tufts were observed. Evaluation of new vessel formation demonstrated that WT and sst$_1$-KO mice did not significantly differ in their median total retinopathy score, with respective values of 4.4 ± 0.33 and of 4.1 ± 0.22 (Fig. 2A). In contrast, the retinopathy score in sst$_2$-KO retinas was significantly higher than in WT or in sst$_1$-KO mice (6.9 ± 0.17; $P <$ 0.01). Similarly (Fig. 2B), no differences between WT and sst$_1$-KO retinas were observed with measurements of the capillary-free area (3.7% ± 0.65% and 4.9% ± 0.44%, respectively), whereas a significant increase by approximately 90% was found in sst$_2$-KO (8.3% ± 0.15%; $P <$ 0.01). A direct comparison between aberrant retinal vessels revealed by fluorescein angiography is shown in the high-resolution, cross-sectional

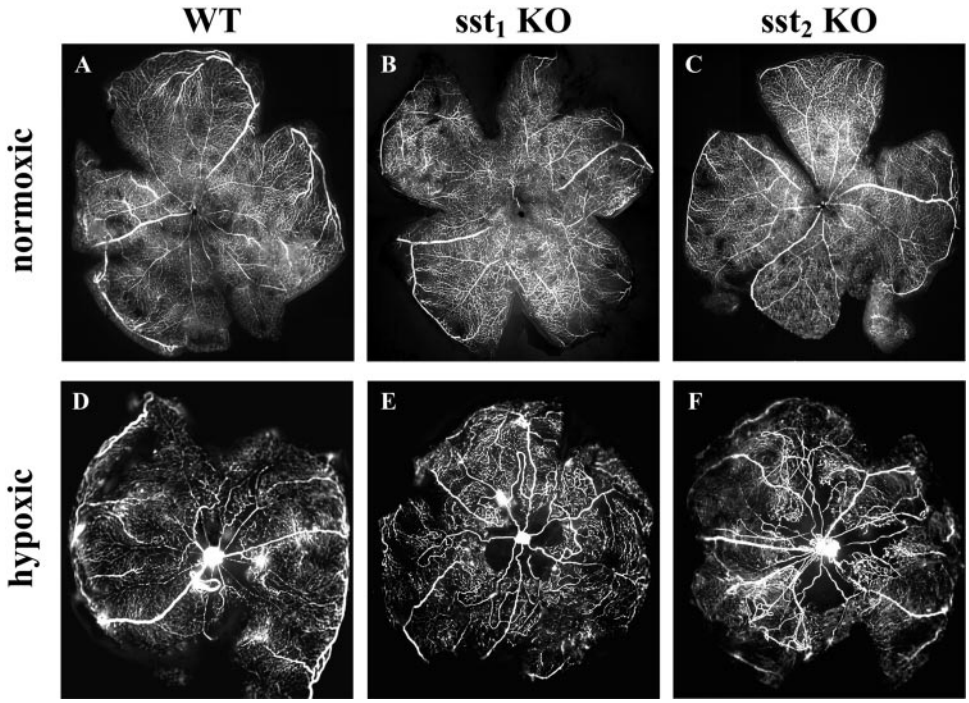

FIGURE 1. Flatmounted retinas perfused with fluorescein-dextran of PD17 WT (**A**, **D**), sst$_1$-KO (**B**, **E**), and sst$_2$-KO (**C**, **F**) mice exposed to room air (**A–C**) or to 75% ± 2% oxygen (**D–F**) from PD7 to PD12. Hyperoxia followed by normoxia for 5 days produced the central loss of blood vessels and the formation of vessel tufts with more evident effects in sst$_2$-KO retinas (**F**) when compared to WT (**D**) and sst$_1$-KO (**E**) retinas. Magnification, ×4.

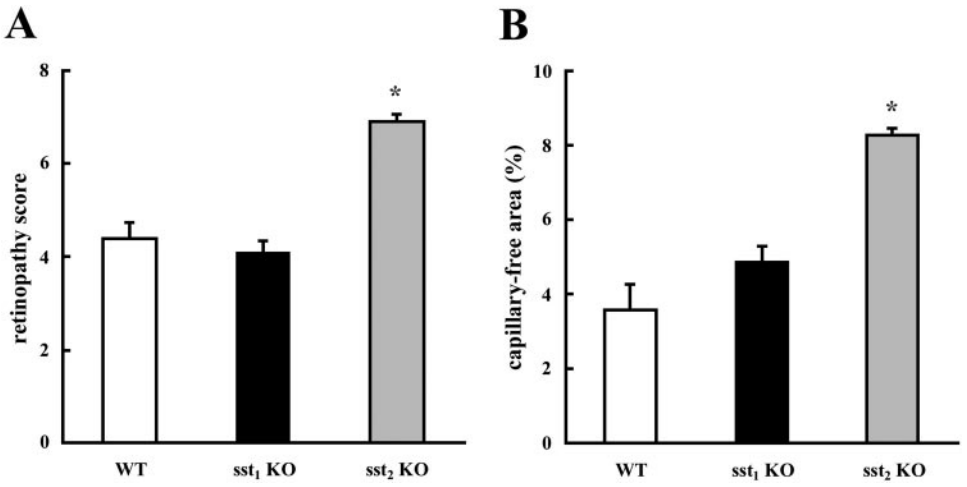

FIGURE 2. Effects of hypoxia on retinal vascularization. (**A**) Retinopathy scores (means ± SE) were significantly higher in sst_2-KO than in WT and sst_1-KO retinas (*$P < 0.01$, ANOVA). (**B**) Capillary-free areas (means ± SE) were significantly higher in sst_2-KO than in WT and sst_1-KO retinas (*$P < 0.01$, ANOVA).

images of retinal vessels in the different strains (Fig. 3). Morphologically similar neovascular tufts extending into the vitreous were observed in all strains.

sst_2 mRNA

Semiquantitative RT-PCR on mouse retina samples yielded amplified products at 76 bp (sst_2). Normoxic and hypoxic retinas had comparable levels of sst_2 mRNA. In the absence of sst_1, sst_2 mRNA was significantly higher (approximately 150%, $P < 0.0001$) than in WT retinas, in agreement with previous results,[27] and was not significantly different from that measured after hypoxia (Fig. 4).

VEGF, VEGFR-1, and VEGFR-2

We determined whether sst_2 overexpression, as in sst_1-KO retinas, or sst_2 deletion was accompanied by alterations in mRNA levels of VEGF, VEGFR-1, and VEGFR-2. RT-PCR yielded amplified products at 221-, 201-, and 198-bp, which correspond to VEGF, VEGFR-1, and VEGFR-2 mRNA, respectively (Figs. 5A–C). Normoxic mRNA levels in WT retinas did not

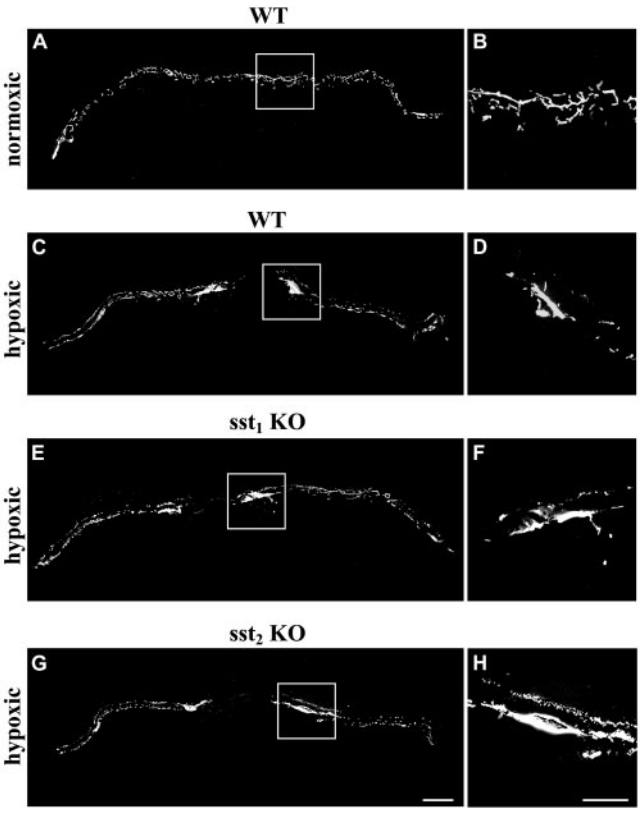

FIGURE 3. Retinal sections cut with a cryostat from the flatmount used for fluorescein angiography. These cross-sectional images show fluorescein-labeled retinal vessels in normoxic WT (**A**), hypoxic WT (**C**), hypoxic sst_1-KO (**E**) and hypoxic sst_2-KO (**G**) retinas. High-power images of the *boxed areas*, representing vascular tufts typical of hypoxic retinas, are in (**B**), (**D**), (**F**), and (**H**), respectively. Scale bars: (**A**, **C**, **E**, **G**) 200 μm; (**B**, **D**, **F**, **H**) 100 μm.

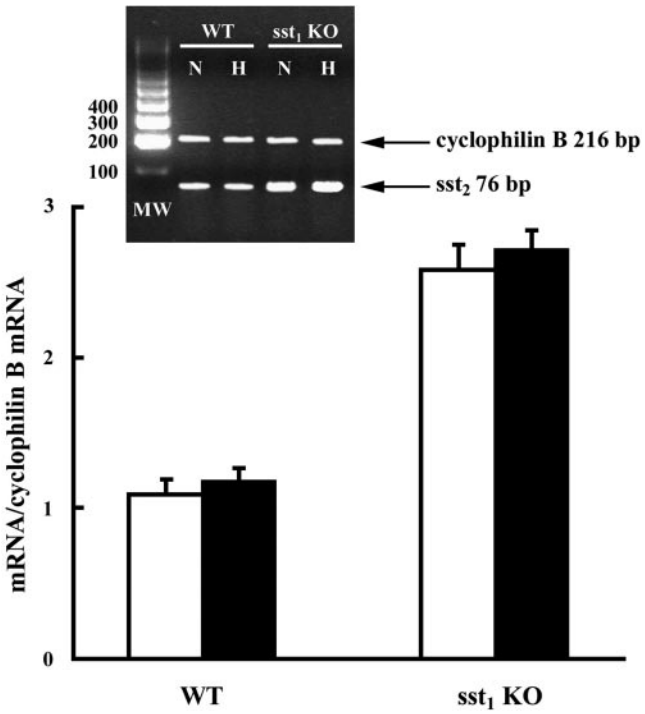

FIGURE 4. Semiquantitative RT-PCR of sst_2 mRNA (band at 76 bp in the *inset*) in both normoxic (□; *lane N* in the *inset*) and hypoxic (■; *lane H* in the *inset*) WT and sst_1-KO retinas. Cyclophilin B mRNA was used as internal standard (band at 216 bp in the *inset*). Hypoxia did not affect sst_2 mRNA in both WT and KO. sst_2 mRNA in sst_1-KO retinas was approximately 150% higher than in WT retinas ($P < 0.0001$; ANOVA). Each column represents the mean ± SE of eight samples. Each sample refers to the mRNA extracted from six retinas.

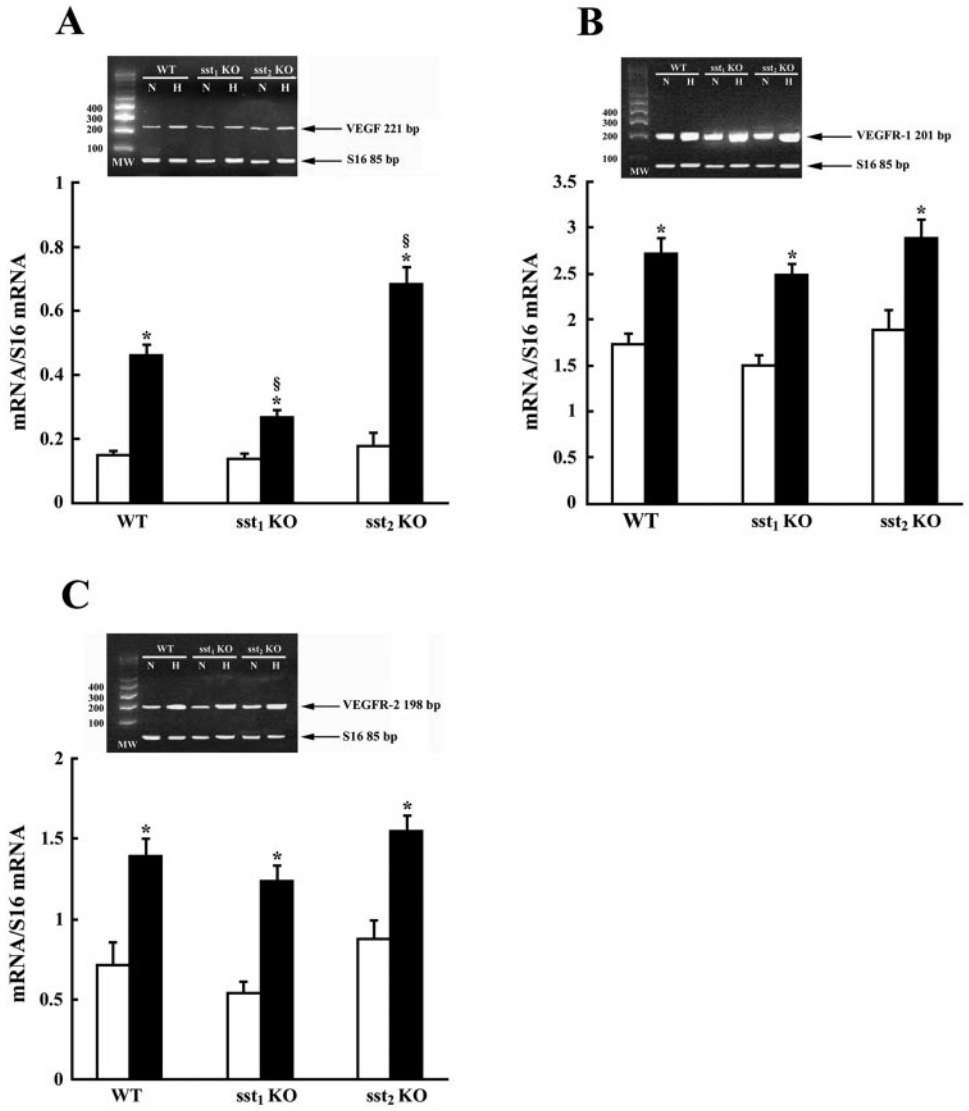

FIGURE 5. Semiquantitative RT-PCR of VEGF mRNA (band at 221 bp in the *inset* in **A**), VEGFR-1 mRNA (band at 201 bp in the *inset* in **B**) and VEGFR-2 mRNA (band at 198 bp in the *inset* in **C**) in both normoxic (□; *lane N* in the *insets*) and hypoxic (■; *lane H* in the *insets*) WT, sst_1-KO, and sst_2-KO retinas. S16 mRNA was used as internal standard (band at 85 bp in the *insets*). (**A**) Normoxic VEGF mRNA did not differ among strains, but it was significantly increased by hypoxia (*$P < 0.01$; ANOVA) to reach a value that was lower in sst_1-KO than in WT retinas (§$P < 0.05$; ANOVA) but higher in sst_2-KO than in WT retinas (§$P < 0.05$; ANOVA). (**B**, **C**) Normoxic levels of both VEGFR-1 mRNA and VEGFR-2 mRNA did not differ among strains but were significantly increased by hypoxia (*$P < 0.01$; ANOVA). Each column represents the mean ± SE of eight samples. Each sample refers to the mRNA extracted from six retinas.

differ significantly from those in KO retinas. In contrast, hypoxia significantly increased ($P < 0.01$) mRNA levels of VEGF (~200%), VEGFR-1 (~55%), and VEGFR-2 (~90%) in all strains. After hypoxia (Fig. 5A), VEGF mRNA was significantly lower in sst_1-KO (~40%, $P < 0.05$) than in WT, but it was significantly higher in sst_2-KO retinas (~50%, $P < 0.05$). The relative levels of VEGF receptor messengers did not differ significantly among strains (Figs. 5B, 5C).

VEGF-immunoreactivity (IR) in normoxic retinas (Fig. 6A) was prominent in cone photoreceptors and in the outer plexiform layer (OPL). Lighter staining was in the ganglion cell layer (GCL) and in the inner nuclear layer (INL) in putative bipolar cells originating processes directed to the inner plexiform layer (IPL). Rare vessels in the inner retina displayed faint VEGF-IR. The same pattern of VEGF-IR was observed in normoxic sst_1-KO and sst_2-KO retinas (data not shown). In WT and in sst_1-KO hypoxic retinas (Figs. 6B, 6C), the overall level of VEGF-IR was consistently increased compared with WT normoxic retinas. In particular, VEGF-IR was more intense in the OPL, in the GCL and in blood vessels. In sst_2-KO hypoxic retinas (Fig. 6D), the increase of VEGF-IR intensity was more pronounced than that in WT or in sst_1-KO retinas.

VEGFR-1-IR was mainly in the OPL of normoxic retinas (Fig. 6E). Photoreceptor outer segments were also immunolabeled. A lighter immunofluorescence was detected in numerous cell somata in the INL and the GCL. Some vessels of the inner retina were also faintly immunolabeled. The immunofluorescence intensity was evidently increased in the vessels as well as in all retinal layers after hypoxia in a similar way in WT (Fig. 6F), sst_1-KO (Fig. 6G), and sst_2-KO (Fig. 6H) retinas compared with the respective normoxic retinas.

VEGFR-2-IR was detected in numerous putative Müller cell processes and in faintly labeled cell bodies within the GCL of normoxic WT retinas (Fig. 6I). Occasional blood capillaries were also lightly labeled. The same pattern was observed in normoxic sst_1- and sst_2-KO retinas (data not shown). In both WT and KO, the immunofluorescence intensity was increased after hypoxia, particularly in the walls of retinal capillaries (Figs. 6J–L). The localization of VEGFR-2-IR to Müller cells was confirmed by the results of double-labeling experiments (Fig. 7A, 7B).

IGF-1 and IGF-1R

RT-PCR on both WT and KO mice yielded amplified products at 351- and 161-bp, which correspond to IGF-1 and IGF-1R mRNA, respectively (Fig. 8). Normoxic IGF-1 mRNA in WT retinas did not differ significantly from that in sst_1-KO retinas, but it was significantly higher than in sst_2-KO ($P < 0.001$, Fig.

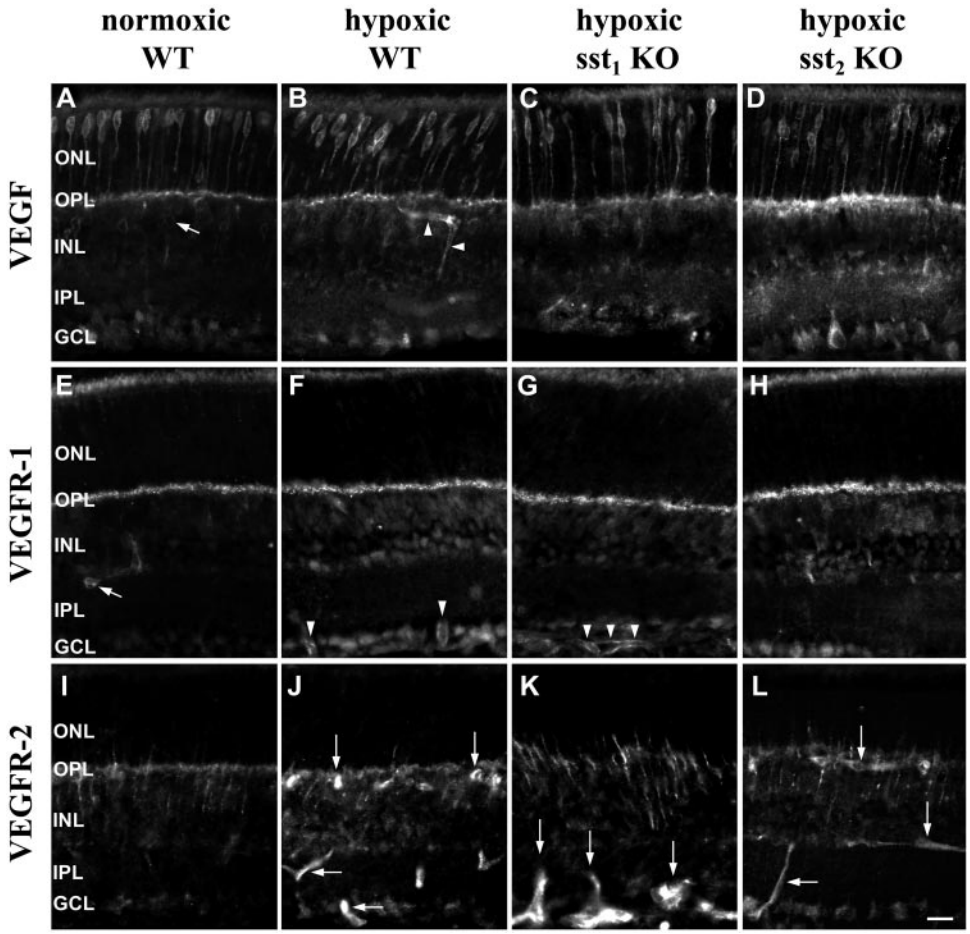

FIGURE 6. Immunohistochemical patterns of VEGF (**A–D**), VEGFR-1 (**E–H**), and VEGFR-2 (**I–L**). In normoxic retinas, there were no apparent differences in the immunohistochemical patterns of WT, sst_1-KO, and sst_2-KO retinas. (**A**) Normoxic, VEGF immunostained WT retina. VEGF immunostaining was in the cone photoreceptors, the outer plexiform layer (OPL), putative bipolar cells (*arrow*), and the ganglion cell layer (GCL). (**B**) Hypoxic WT retina. The overall VEGF immunofluorescence intensity was higher than in the normoxic retina. VEGF immunostaining became clearly visible in several retinal capillaries (*arrowheads*). (**C**, **D**) Hypoxic sst_1-KO and sst_2-KO retinas, respectively. The increase in immunofluorescence intensity was particularly evident in the OPL and in the GCL of the sst_2-KO retinas (**D**). (**E**) Normoxic, VEGFR-1-immunostained WT retina. VEGFR-1 immunostaining was mainly in the OPL and in lightly stained blood vessels (*arrow*). In hypoxic WT (**F**), sst_1-KO (**G**), and sst_2-KO (**H**) retinas, the VEGFR-1 immunostaining became evident in the inner nuclear layer (INL) and GCL and in the walls of retinal capillaries (**F**, **G**, *arrowheads*). (**I**) Normoxic, VEGFR-2-immunostained WT retina. VEGFR-2 immunostaining was mainly in vertically directed processes probably belonging to Müller glial cells and in faintly stained cells in the GCL. In hypoxic WT (**J**), sst_1-KO (**K**) and sst_2-KO (**L**) retinas, the VEGFR-2 immunofluorescence intensity increased. In particular, blood vessels became highly immunostained (**J–L**, *arrows*). Scale bar, 20 μm.

8A). In both WT and sst_1-KO, hypoxia did not affect IGF-1 mRNA which was, in contrast, increased by approximately threefold in sst_2-KO retinas ($P < 0.001$), reaching a level similar to that in WT and sst_1-KO. In both WT and KO retinas, hypoxia significantly increased IGF-1R mRNA ($P < 0.01$). IGF-1R mRNA was significantly lower in sst_1-KO ($\sim$40%, $P < 0.05$) than in WT retinas after hypoxia, whereas IGF-1R mRNA was significantly higher in sst_2-KO ($\sim$40%, $P < 0.05$) than in WT (Fig. 8B).

As depicted in Figures 9A–D, IGF-1-IR was detected in all retinal layers, and it was prominent in the OPL and in GCL somata. In the outer nuclear layer (ONL), it was detected in Müller cell processes, as confirmed by double-labeling experiments (Figs. 7C, 7D). In normoxic retinas, the IGF-1 staining in the WT (Fig. 9A, left) was similar to that in sst_1-KO retinas (data not shown). In contrast, the immunofluorescence intensity was drastically reduced in sst_2-KO retinas, where it appeared unchanged in the OPL, but it was markedly reduced in all other retinal layers (Fig. 9A, right). In hypoxic retinas of all strains, the immunostaining pattern was similar to that in normoxic WT retinas (Figs. 9B–D).

In normoxic retinas (Fig. 9E), IGF-1R-IR was prominent in the OPL and sparse throughout the IPL. The outline of several somata in the mid-distal INL showed light immunostaining. In addition, IGF-1R-expressing Müller cells were also detected as confirmed by double-labeling experiments (Figs. 7E, 7F). Retinal capillaries did not display IGF-1R-IR. The same pattern was observed in normoxic sst_1-KO and sst_2-KO retinas (data not shown). In hypoxic retinas of WT, sst_1-KO, and sst_2-KO mice, the IGF-1R immunofluorescence intensity was dramatically increased in all retinal layers, particularly in the IPL and in Müller cell processes (Figs. 9F–H).

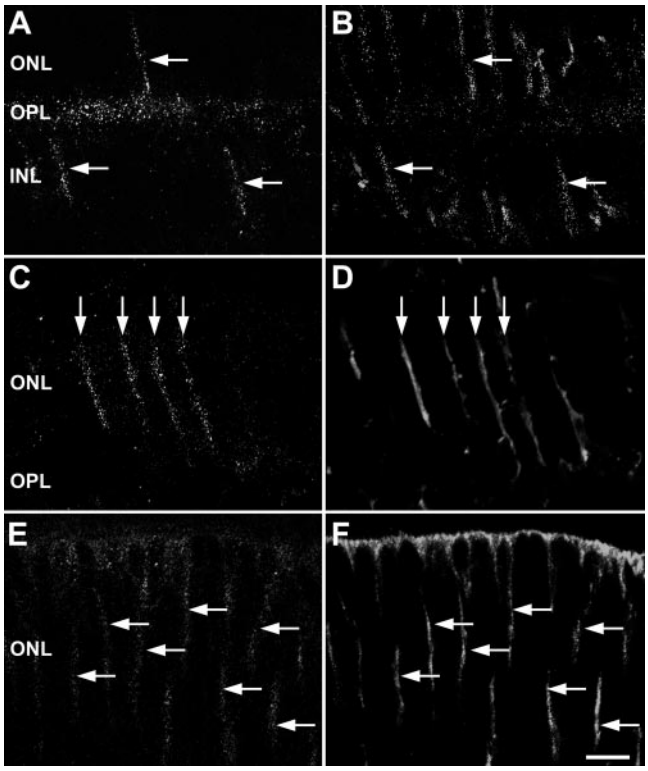

FIGURE 7. Double-labeling experiments showing expression of VEGFR-2, IGF-1, and IGF-1R in Müller cells labeled with glutamine synthetase antibodies. (**A**) VEGFR-2 immunostaining. (**B**) The same field as in (**A**) showing glutamine synthetase immunolabeling. (**C**) IGF-1 immunostaining. (**D**) The same field as in (**C**) showing glutamine synthetase immunolabeling. (**E**) IGF-1R immunostaining. (**F**) the same field as in (**E**) showing glutamine synthetase immunolabeling. *Arrows*: double-Labeled Müller cell processes. INL, inner nuclear layer; ONL, outer nuclear layer; OPL, outer plexiform layer. Scale bar, 10 μm.

Ang/Tie mRNA

RT-PCR yielded amplified products at 278-, 375-, 363- and 253-bp, which correspond to Ang-1, Ang-2, Tie-1, and Tie-2 mRNA, respectively (Figs. 10A–D). Normoxic mRNA levels in WT retinas did not differ significantly from those in KO retinas except for Ang-2 mRNA, which was significantly higher (~15%) in sst_2-KO than in WT ($P < 0.0001$), and Tie-2 mRNA, which was significantly higher (~40%) in both sst_1- and sst_2-KO than in WT ($P < 0.0001$) retinas. Hypoxia did not affect Ang-1 mRNA in either WT or sst_1-KO retinas, whereas it significantly decreased Ang-1 mRNA (~20%) in sst_2-KO ($P < 0.01$). In contrast, hypoxia significantly increased ($P < 0.00001$) mRNA levels of Ang-2 (~20%) in both WT and sst_1-KO retinas, but not in sst_2-KO. Tie-1 mRNA was not influenced by hypoxia in WT, whereas it was either increased (~20%, $P < 0.001$) in sst_1-KO or decreased (~45%, $P < 0.00001$) in sst_2 KO. After hypoxia, Tie-2 mRNA increased significantly in WT (~15%, $P < 0.01$), remained unchanged in sst_1-KO and decreased significantly in sst_2-KO (~30%, $P < 0.00001$) retinas.

DISCUSSION

In this study, we report findings regarding the function of sst_2 in the control of angiogenesis and its associated factors in a model of hypoxia-induced retinal neovascularization in transgenic mice with altered sst_2 levels in the retina.[23,25,27] Our hypothesis that modulation of sst_2 may provide an effective mechanism for regulation of retinal neovascularization has been satisfied, at least in part. Indeed, although a chronic overexpression of sst_2 (as in sst_1-KO retinas) did not attenuate retinal neovascularization, the lack of sst_2 was associated with significantly worsened neovascularization. We also show that sst_2 levels in the retina differentially influenced angiogenesis-associated factors, thus indicating a strain-dependent expression of these factors that may determine heterogeneity in the angiogenic response and, potentially, susceptibility to angiogenesis-dependent diseases.

Effects of Hypoxia on Angiogenesis-Associated Growth Factors

As shown by our results in WT mice, both the expression of VEGF and its receptors and that of the proangiogenic factor Ang-2 and its receptor Tie-2, increased as a result of hypoxia, in agreement with previous observations.[7,11,12,35,36] The fact that hypoxia did not influence Ang-1 is in line with previous results in human retinas with ischemia-induced neovascularization,[37] although a slight increase in Ang-1 expression has been re-

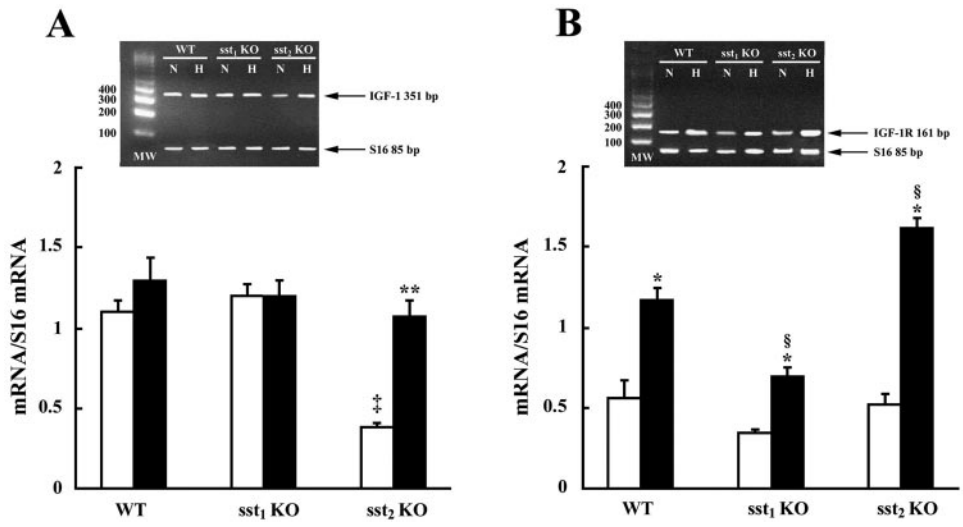

FIGURE 8. Semiquantitative RT-PCR of IGF-1 mRNA (band at 351 bp in the *inset* in **A**) and IGF-1R mRNA (band at 161 bp in the *inset* in **B**) in both normoxic (□; *lane N* in the *insets*) and hypoxic (■; *lane H* in the *insets*) WT, sst_1-KO, and sst_2-KO retinas. S16 mRNA was used as the internal standard (band at 85 bp in the *insets*). (**A**) Normoxic levels of IGF-1 mRNA were similar in WT and sst_1-KO whereas IGF-1 mRNA in sst_2-KO retinas was significantly lower than in WT and sst_1-KO (‡$P < 0.001$; ANOVA). Hypoxia did not affect IGF-1 mRNA in both WT and sst_1-KO retinas, whereas IGF-1 mRNA in sst_2-KO retinas was significantly higher than in normoxia (**$P < 0.001$; ANOVA). (**B**) Normoxic levels of IGF-1R mRNA did not differ among strains. They were significantly increased by hypoxia (*$P < 0.01$; ANOVA), reaching a level that was significantly lower in sst_1-KO than in WT (§$P < 0.05$; ANOVA), but significantly higher in sst_2-KO than in WT retinas (§$P < 0.05$; ANOVA). Each column represents the mean ± SE of eight samples. Each sample refers to the mRNA extracted from six retinas.

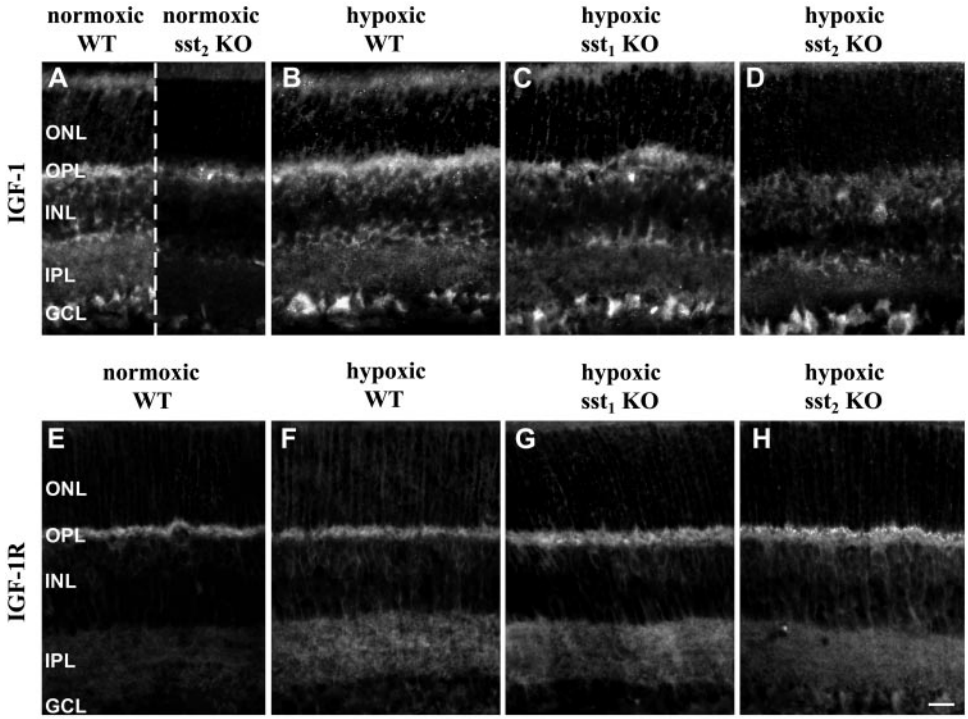

FIGURE 9. Immunohistochemical patterns of IGF-1 (**A–D**) and IGF-1R (**E–H**). (**A**) Normoxic, IGF-1-immunostained WT retina (*left*) and normoxic, IGF-1-immunostained sst_2-KO retina (*right*). IGF-1-IR was evident in the outer plexiform layer (OPL) and in the ganglion cell layer (GCL). IGF-1-IR was also in putative Müller cell processes in the outer nuclear layer (ONL). The immunofluorescence intensity was drastically reduced in the sst_2-KO retina. In hypoxic WT (**B**), sst_1-KO (**C**) and sst_2-KO (**D**) retinas, the IGF-1 immunostaining pattern was similar to that in normoxic WT retinas. (**E**) Normoxic, IGF-1R-immunostained WT retina. IGF-1R immunostaining was prominent in the OPL and faint in the inner plexiform layer (IPL). Cells in the distal inner nuclear layer (INL) and putative Müller cell processes were also labeled. In hypoxic WT (**F**), sst_1-KO (**G**) and sst_2-KO (**H**) retinas, the IGF-1R immunofluorescence intensity was increased in all retinal layers. Scale bar, 20 μm.

ported in hypoxic mouse retinas.[11] Our results also demonstrate that retinal IGF-1 mRNA did not change after hypoxia, whereas the expression of IGF-1R significantly increased, in agreement with previous results demonstrating increased levels of retinal IGF-1R mRNA, but not of IGF-1 mRNA, in hypoxic rat retinas.[38] That neovascularization is not associated with

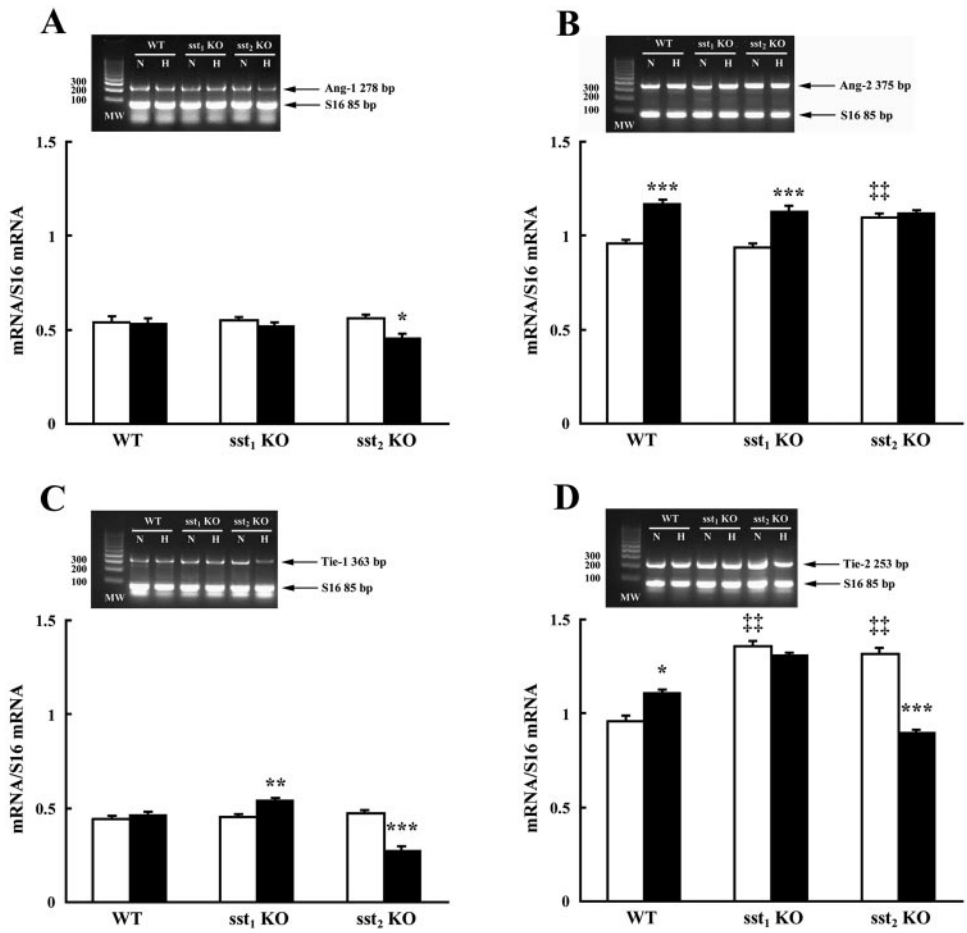

FIGURE 10. Semiquantitative RT-PCR of Ang-1 mRNA (band at 278 bp in the *inset* in **A**), Ang-2 mRNA (band at 375 bp in the *inset* in **B**), Tie-1 mRNA (band at 363 bp in the *inset* in **C**), and Tie-2 mRNA (band at 253 bp in the *inset* in **D**) in both normoxic (□; *lane N* in the *insets*) and hypoxic (■; *lane H* in the *insets*) WT, sst_1-KO, and sst_2-KO retinas. S16 mRNA was used as internal standard (band at 85 bp in the *insets*). (**A**) Ang-1 mRNA was not affected by hypoxia except for showing a significant decrease in sst_2-KO retinas ($^*P < 0.01$; ANOVA). (**B**) Ang-2 mRNA was significantly increased by hypoxia in both WT and sst_1-KO ($^{***}P < 0.00001$; ANOVA). Normoxic level of Ang-2 mRNA in sst_2-KO retinas was significantly higher than in WT and sst_1-KO ($‡‡P < 0.0001$; ANOVA) and comparable to that measured after hypoxia. (**C**) Hypoxia significantly increased Tie-1 mRNA in sst_1-KO ($^{**}P < 0.001$; ANOVA) whereas significantly decreased Tie-1 mRNA in sst_2-KO ($^{***}P < 0.00001$; ANOVA). (**D**) Normoxic levels of Tie-2 mRNA in KO were significantly higher than in WT ($‡‡P < 0.0001$; ANOVA). Hypoxia significantly increased the level of Tie-2 mRNA in WT ($^*P < 0.01$; ANOVA), did not affect Tie-2 mRNA in sst_1-KO, whereas it significantly decreased Tie-2 mRNA in sst_2-KO ($^{***}P < 0.00001$; ANOVA). Each column represents the mean ± SE of eight samples. Each sample refers to the mRNA extracted from six retinas.

altered IGF-1 mRNA has also been recently demonstrated in different models of retinopathy in mice.[8,9]

Influence of sst_2 Levels on Angiogenesis-Associated Growth Factors

Our results demonstrate that enhanced somatostatinergic function at sst_2 limited the hypoxia-induced VEGF increase, whereas sst_2 loss upregulated this increase. Thus, sst_1-KO retinas were protected to some extent from hypoxia which, in contrast, had a more serious influence after sst_2 loss. An SRIF-induced regulation of VEGF has been suggested,[16,18] although there are also studies demonstrating that SRIF does not influence VEGF levels, as it does GH or IGF-1.[39] Our additional finding that sst_2 loss upregulated the hypoxia-induced increase of IGF-1R mRNA suggests the possibility that sst_2 may regulate VEGF expression through an increased expression of IGF-1R. In this respect, results from human RPE cells demonstrate that activation of sst_2 inhibits IGF-1R phosphorylation and the downstream VEGF synthesis.[16] Our finding that normoxic levels of IGF-1 mRNA were drastically decreased by sst_2 loss is difficult to explain, since activation of sst_2 is known to decrease IGF-1.[17] One possibility is that sst_2 loss causes excessive stimulation of IGF-1R which would in turn elicit feedback mechanisms to decrease IGF-1 expression. These mechanisms would be removed in hypoxia, as we observed that, in the absence of sst_2, IGF-1 mRNA expression was enhanced, and it reached levels that were comparable to those in WT or in sst_1-KO retinas. As also shown by our results, sst_2 levels appeared to influence the effects of hypoxia on the Ang/Tie system. Ang-1, acting on Tie-2, is known to promote vascular integrity and maturation, whereas Ang-2 is an antagonist of Ang-1 and promotes VEGF-induced proliferation of endothelial cells.[40] In addition, Tie-1 promotes structural integrity of endothelial cells.[41] We found that, after hypoxia, Ang-1, Tie-1, and Tie-2 mRNAs were decreased in the absence of sst_2, whereas Tie-1 mRNA was increased when sst_2 was overexpressed, as in sst_1-KO retinas. Together, these results add further evidence to the possibility that sst_2 may be beneficial in limiting hypoxia-induced neovascularization in the retina.

Immunohistochemical Observations

Our immunohistochemical observations are consistent with the data of mRNA expression as evaluated with RT-PCR. Of interest, in WT as well as in KO retinas, the hypoxia-induced increase of VEGFR-1 and -2 mRNA is paralleled by a pronounced increase of VEGFR-1 and -2 immunolabel intensity in retinal vessels, consistent with a direct action exerted by VEGF on retinal vessels in hypoxic conditions.[36] In addition, the hypoxia-induced increase in VEGF immunofluorescence intensity is more pronounced in sst_2-KO than in WT or in sst_1-KO retinas, thus implementing our data on effects of sst_2 loss on retinal neovascularization.

Although localization of VEGF, IGF-1 and their receptors to retinal cells is still controversial, and different retinal patterns of immunohistochemical or in situ hybridization labeling have been reported in different species,[2–6,42–44] our immunohistochemical results demonstrate that these molecules are predominantly expressed by neuronal elements and glial cells and only to a minor extent by retinal vessels. In particular, VEGFR-2, IGF-1, and IGF-1R have been localized to Müller cells in agreement with previous results.[45] Our observation of IGF-1 localization to Müller cells is in agreement with reports of these cells as an important source of retinal IGF-1.[6,46] In addition, a substantial body of information suggests that Müller cells are involved in proliferative diabetic retinopathy.[47] Finally, the localization of angiogenesis-associated factors to retinal neural and glial elements is in agreement with proposed functions of these factors that may be related to neuronal survival.[48–50]

Conclusion

The present study demonstrates that sst_2 exerts protective effects against retinal neoangiogenesis and suggests that sst_2 agonists are useful in retinal diseases characterized by neovascularization. The immediate clinical importance lies in the establishment of a potential pharmacologic target based on sst_2 pharmacology.

Acknowledgments

The authors thank Angelo Gazzano and Gino Bertolini (University of Pisa, Italy) for assistance with mouse colonies.

References

1. Gariano RF, Gardner TW. Retinal angiogenesis in development and disease. *Nature*. 2005;438:960–966.
2. McLeod DS, Taomoto M, Cao J, Zhu Z, Witte L, Lutty GA. Localization of VEGF receptor-2 (KDR/Flk-1) and effects of blocking it in oxygen-induced retinopathy. *Invest Ophthalmol Vis Sci*. 2002;43:474–482.
3. Gilbert RE, Vranes D, Berka JL, et al. Vascular endothelial growth factor and its receptors in control and diabetic rat eyes. *Lab Invest*. 1998;78:1017–1027.
4. Burren CP, Berka JL, Edmondson SR, Werther GA, Batch JA. Localization of mRNAs for insulin-like growth factor-I (IGF-I), IGF-I receptor, and IGF binding proteins in rat eye. *Invest Ophthalmol Vis Sci*. 1996;37:1459–1468.
5. Lutty GA, McLeod DS, Merges C, Diggs A, Plouet J. Localization of vascular endothelial growth factor in human retina and choroid. *Arch Ophthalmol*. 1996;114:971–977.
6. Charkrabarti S, Ghahary A, Murphy LJ, Sima AA. Insulin-like growth factor-I expression is not increased in the retina of diabetic BB/W-rats. *Diabetes Res Clin Pract.* 1991;14:91–97.
7. Werdich XQ, McCollum GW, Rajaratnam VS, Penn JS. Variable oxygen and retinal VEGF levels: correlation with incidence and severity of pathology in a rat model of oxygen-induced retinopathy. *Exp Eye Res*. 2004;79:623–630.
8. Leske DA, Wu J, Mookadam M, et al. The relationship of retinal VEGF and retinal IGF-1 mRNA with neovascularization in an acidosis-induced model of retinopathy of prematurity. *Curr Eye Res*. 2006;31:163–169.
9. Leske DA, Wu J, Fautsch MP, et al. The role of VEGF and IGF-1 in a hypercarbic oxygen-induced retinopathy rat model of ROP. *Mol Vis*. 2004;10:43–50.
10. Kuang H, Zou W, Liu D, et al. The potential role of IGF-I receptor mRNA in rats with diabetic retinopathy. *Chin Med J*. 2003;116:478–480.
11. Kociok N, Krohne TU, Poulaki V, Joussen AM. Geldanamycin treatment reduces neovascularization in a mouse model of retinopathy of prematurity. *Graefes Arch Clin Exp Ophthalmol*. 2007;245:258–266.
12. Park YS, Kim NH, Jo I. Hypoxia and vascular endothelial growth factor acutely up-regulate angiopoietin-1 and Tie1 mRNA in bovine retinal pericytes. *Microvasc Res*. 2003;65:125–131.
13. Saharinen P, Kerkela K, Ekman N, et al. Multiple angiopoietin recombinant proteins activate the Tie1 receptor tyrosine kinase and promote its interaction with Tie2. *J Cell Biol*. 2005;169:239–243.
14. Missotten T, Baarsma GS, Kuijpers RW, et al. Somatostatin-related therapeutics in ophthalmology: a review. *J Endocrinol Invest*. 2005;28:118–126.
15. Dasgupta P. Somatostatin analogues: multiple roles in cellular proliferation, neoplasia, and angiogenesis. *Pharmacol Ther*. 2004;102:61–85.
16. Sall JW, Klisovic DD, O'Dorisio MS, Katz SE. Somatostatin inhibits IGF-1 mediated induction of VEGF in human retinal pigment epithelial cells. *Exp Eye Res*. 2004;79:465–476.

17. Garcia de la Torre N, Wass JA, Turner HE. Antiangiogenic effects of somatostatin analogues. *Clin Endocrinol.* 2002;57:425–441.
18. Baldysiak-Figiel A, Lang GK, Kampmeier J, Lang GE. Octreotide prevents growth factor-induced proliferation of bovine retinal endothelial cells under hypoxia. *J Endocrinol*. 2004;180:417–424.
19. Higgins MD, Yan Y, Schrier BK. Somatostatin analogs inhibit neonatal retinal neovascularization. *Exp Eye Res*. 2002;74:553–559.
20. Grant MB, Caballero S Jr. The potential role of octreotide in the treatment of diabetic retinopathy. *Treat Endocrinol*. 2005;4:199–203.
21. Allen JP, Hathway GJ, Clarke NJ, et al. Somatostatin receptor 2 knockout/lacZ knockin mice show impaired motor coordination and reveal sites of somatostatin action within the striatum. *Eur J Neurosci.* 2003;17:1881–1895.
22. Kreienkamp HJ, Akgun E, Baumeister H, Meyerhof W, Richter D. Somatostatin receptor subtype 1 modulates basal inhibition of growth hormone release in somatotrophs. *FEBS Lett*. 1999;462:464–466.
23. Casini G, Catalani E, Dal Monte M, Bagnoli P. Functional aspects of the somatostatinergic system in the retina and the potential therapeutic role of somatostatin in retinal disease. *Histol Histopathol*. 2005;20:615–632.
24. Bigiani A, Petrucci C, Ghiaroni V, et al. Functional correlates of somatostatin receptor 2 overexpression in the retina of mice with genetic deletion of somatostatin receptor 1. *Brain Res*. 2004;1025:177–185.
25. Casini G, Dal Monte M, Petrucci C, et al. Altered morphology of rod bipolar cell axonal terminals in the retinas of mice carrying genetic deletion of somatostatin subtype receptor 1 or 2. *Eur J Neurosci.* 2004;19:43–54.
26. Pavan B, Fiorini S, Dal Monte M, et al. Somatostatin coupling to adenylyl cyclase activity in the mouse retina. *Naunyn Schmiedebergs Arch Pharmacol.* 2004;370:91–98.
27. Dal Monte M, Petrucci C, Vasilaki A, et al. Genetic deletion of somatostatin receptor 1 alters somatostatinergic transmission in the mouse retina. *Neuropharmacology*. 2003;45:1080–1092.
28. Dal Monte M, Petrucci C, Cozzi A, Allen JP, Bagnoli P. Somatostatin inhibits potassium-evoked glutamate release by activation of the sst_2 somatostatin receptor in the mouse retina. *Naunyn Schmiedebergs Arch Pharmacol.* 2003;367:188–192.
29. Smith LEH, Wesolowski E, McLellan A, et al. Oxygen-induced retinopathy in the mouse. *Invest Ophthalmol Vis Sci*. 1994;35:101–111.
30. D'Amato R, Wesolowski E, Smith LE. Microscopic visualization of the retina by angiography with high-molecular-weight fluorescein-labeled dextrans in the mouse. *Microvasc Res*. 1993;46:135–142.
31. Higgins RD, Yu K, Sanders RJ, Nandgaonkar BN, Rotschild T, Rifkin DB. Diltiazem reduces retinal neovascularization in a mouse model of oxygen induced retinopathy. *Curr Eye Res*. 1999;18:20–27.
32. Rozen S, Skaletsky H. Primer3 on the WWW for general users and for biologist programmers. *Methods Mol Biol*. 2000;132:365–386.
33. Ida H, Tobe T, Nambu H, Matsumura M, Uyama M, Campochiaro PA. RPE cells modulate subretinal neovascularization, but do not cause regression in mice with sustained expression of VEGF. *Invest Ophthalmol Vis Sci*. 2003;44:5430–5437.
34. Linser P, Moscona AA. Induction of glutamine synthetase in embryonic neural retina: localization in Müller fibers and dependence on cell interactions. *Proc Natl Acad Sci USA*. 1979;76:6476–6480.
35. Noda K, Ishida S, Shinoda H, et al. Hypoxia induces the expression of membrane-type 1 matrix metalloproteinase in retinal glial cells. *Invest Ophthalmol Vis Sci*. 2005;46:3817–3824.
36. Witmer AN, Vrensen GFJM, Van Noorden CJF, Schlingemann RO. Vascular endothelial growth factors and angiogenesis in eye disease. *Prog Retin Eye Res*. 2003;22:1–29.
37. Takagi H, Koyama S, Seike H, et al. Potential role of angiopoietin/Tie2 system in ischemia-induced retinal neovascularization. *Invest Ophthalmol Vis Sci*. 2003;44:393–402.
38. Averbukh E, Weiss O, Halpert M, et al. Gene expression of insulin-like growth factor-I, its receptor and binding proteins in retina under hypoxic conditions. *Metabolism*. 1998;47:1331–1336.
39. Lawnicka H, Stepien H, Wiczolkowska J, Kolago B, Kunert-Radek J, Komorowski J. Effect of somatostatin and octreotide on proliferation and vascular endothelial growth factor secretion from murine endothelial cell line (HECa10) culture. *Biochem Biophys Res Commun*. 2000;268:567–571.
40. Kobayashi H, Lin PC. Angiopoietin/Tie2 signaling, tumor angiogenesis and inflammatory diseases. *Front Biosci*. 2005;10:666–674.
41. Sato T, Tozawa Y, Deutsch U, et al. Distinct roles of the receptor tyrosine kinases Tie-1 and Tie-2 in blood vessel formation. *Nature*. 1995;376:70–74.
42. Feeney SA, Simpson DA, Gardiner TA, Boyle C, Jamison P, Stitt AW. Role of vascular endothelial growth factor and placental growth factors during retinal vascular development and hyaloid regression. *Invest Ophthalmol Vis Sci*. 2003;44:839–847.
43. Blaauwgeers HG, Holtkamp GM, Rutten H, et al. Polarized vascular endothelial growth factor secretion by human retinal pigment epithelium and localization of vascular endothelial growth factor receptors on the inner choriocapillaris: evidence for a trophic paracrine relation. *Am J Pathol*. 1999;155:421–428.
44. Ocrant I, Valentino KL, King MG, Wimpy TH, Rosenfeld RG, Baskin DG. Localization and structural characterization of insulin-like growth factor receptors in mammalian retina. *Endocrinology*. 1989;125:2407–2413.
45. Shaw LC, Pan H, Afzal A, et al. Proliferating endothelial cell-specific expression of IGF-I receptor ribozyme inhibits retinal neovascularization. *Gene Ther*. 2006;13:752–760.
46. Li F, Cao W, Steinberg RH, LaVail MM. BasicFGF-induced down-regulation of IGF-I mRNA in cultured rat Müller cells. *Exp Eye Res*. 1999;68:19–27.
47. Guidry C. The role of Müller cells in fibrocontractive retinal disorders. *Prog Retin Eye Res*. 2005;24:75–86.
48. Jin KL, Mao XO, Greenberg DA. Vascular endothelial growth factor: direct neuroprotective effect in in vitro ischemia. *Proc Natl Acad Sci USA*. 2000;97:10242–10247.
49. Sondell M, Sundler F, Kanje M. Vascular endothelial growth factor is a neurotrophic factor which stimulates axonal outgrowth through the flk-1 receptor. *Eur J Neurosci*. 2000;12:4243–4254.
50. Politi LE, Rotstein NP, Salvador G, Giusto NM, Insua MF. Insulin-like growth factor-I is a potential trophic factor for amacrine cells. *J Neurochem*. 2001;76:1199–1211.